Application of the Singular Spectrum Analysis to the time variations of the amplitude of Schumann resonance measurements

1st Jesús Rodríguez-Camacho
University of Granada
Granada, Spain
jesrodcam@ugr.es

2th David Blanco-Navarro
University of Granada
Granada, Spain
dblanco@ugr.es

3th Juan Francisco Gómez-Lopera
University of Granada
Granada, Spain
jfgomez@ugr.es

4th Mª Carmen Carrión
University of Granada
Granada, Spain
mcarrion@ugr.es

***Abstract*—The Singular Spectrum Analysis technique has been applied to the amplitude of the first Schumann resonance measured at the Sierra Nevada station (Spain) in order to obtain the principal components of its time evolution. The results of this study confirm the appearance of the annual and semiannual components that have been pointed out for this resonance and also reveal other components corresponding to 45 to 120 days variations, which matches the variations of athmospheric waves like the Madden-Julian oscillation and the Kelvin waves. A preprocessing of the measurements is required since the station has experienced some technical failures and there are thus some gaps in the measured data. The application of the technique has been made taking one data per month and one data per day, and the results have been compared.**

***Index Terms*—Schumann resonance, Singular Spectrum Analysis, Principal Components**

I. Introduction

The electromagnetic cavity delimited by the surface of the Earth and the lower ionosphere is continuously excited by lightning events, which leads to the appearance of natural electromagnetic field waves. The Extremely Low Frequency (ELF) component of these waves is called Schumann Resonance (SR). This resonance was first predicted by W. O. Schumann in 1952, and was first measured by Balser and Wagner in 1960 [1]. It has the interesting feature that it is a global phenomenon, in the sense that the SR measured in a specific location of the globe will provide information about the whole Earth-ionosphere cavity, and not only about the area surrounding the measurement station. The SR has relevant application to many different scientific problems. Some examples are the study of the biological impact of this resonance in heart cells [2] or in the evolution of hospital admissions [3], the inversion problem that tries to find out the global thunderstorm distribution from the SR measurements in different locations of the world [4], or the predictions of earthquakes [5].

An ELF measurement station was designed and built in Sierra Nevada, Spain (37°02′N, 3°19′W) to study this phenomenon [6]. This station comprises two horizontal magnetometers in the North-South and East-West directions, respectively, and has been calibrated to work in the band 6-25 Hz, where the first three resonances can be found (in the approximate frequencies of 8, 14 and 20 Hz). The first recordings of the station date from March 2013, and there have been some short periods of interruption since them.

Due to its global definition, any change in the ionosphere or in the lightning distribution around the world may affect the SR recordings and thus may be responsible for the variations observed. It is convenient to separate the different scale variations that are observed in a series of SR recordings for a better understanding of the phenomenon and its relation to other natural, atmospheric and environmental phenomena. In particular, a study of the relation between the SR and some well-known atmospheric waves like the Madden-Julian oscillation or the Kelvin waves is currently being carried out [7].

In order to obtain the principal components of the time variations of the SR, the Singular Spectrum Analysis (SSA) will be used. The origin of this technique is attributed to Broomhead and King [8] and it has been described and applied to many different problems since then [9]. The aim of the SSA technique is the decomposition of an original series into the sum of a small number of independent and interpretable components [9].

This work has been supported by the Ministry of Education, Science and Sport of Spain through the FPU grants for PhD studentship (reference: FPU15/04291). This work has also been supported by the Ministry of Economy and Competitiveness of Spain under the project with reference FIS2017-90102-R, co-financed with FEDER funds of the EU.

II. Preprocessing of the SR recordings

The raw horizontal magnetic field recordings are processed in order to obtain the SR parameter values as explained in [10] and [11]. The first step of the processing is to apply the Welch method in order to obtain the amplitude spectra of each 10-minute interval recording of raw data. The second step is to perform a Lorentzian fit on the spectra to extract the quantitative values of the parameters (amplitude, central frequency and width) from the spectra, as shown in Fig. 1. After this, one value of each parameter is available for every interval of 10 minutes. The study of the regular variations and the anomalous observations is usually the first step to correlate the SR measurements with other phenomena. A description on how this study is carried out with the Sierra Nevada recordings can be found in [12].

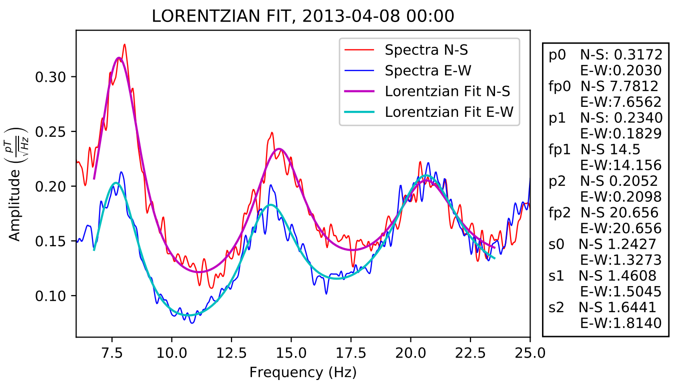

Fig. 1. Amplitude spectra of the NS and EW components of the horizontal magnetic field recorded at the Sierra Nevada station from the 7th of April 2013 at 23:55:00 to the 8th of April 2013 at 00:05:00, together with the Lorentzian fits. The value of the amplitudes (p_i), central frequencies (fp_i) and widths (s_i) for this 10-minute interval are shown on the right.

In order to apply the SSA technique on the time series of the first resonance amplitude values, it is needed to fill the data gaps that appear as a consequence of technical failures of the Sierra Nevada measurement station. These gaps may last for 10 minutes (only one missing value) or for several weeks (even up to 10 weeks) for serious failures, as shown in Fig. 2a. The percentage of time intervals for which there are no recordings is approximately 5%. In order to fill these gaps, we take into consideration the data both in a similar date and at a similar hour to the missing data. The closer a recording is to a missing interval, the more it will be taken into account for the prediction. The relative importance that will be given for the close recordings to predict the value of a missing interval is shown in Fig. 3. The filled time series for the first SR amplitude is shown in Fig. 2b.

III. Application of the Singular Spectrum Analysis to the time series of the first SR amplitude

The length of the data series used to extract the principal components is 5 years (from 1 March 2013 to 28 February 2018). The application of the SSA technique will be made first taking one sample per month, and secondly taking one sample per day. When taking one sample per month, the total number of samples of the series is $T = 60$, and when taking one sample per day, it is $T = 1826$.

Following the notation of [9], the time series of the first SR amplitude will be denoted $Y = (y_1, ..., y_T)$, and a number of K series $X_1, ..., X_K$ will be obtained by lagging the vector Y, $X_i = (y_i, y_{i+1}, ..., y_{i+L-1})$, for $i \in \{1, ..., K\}$, where the condition $K = T - L + 1$ is satisfied. In our case, $L = 24$ and $K = 37$ have been established when taking one sample per month, while $L = 730$ and $K = 1097$ when taking one sample per day. We must consider the matrix $X = [X_1, ..., X_K]$:

$$X = \begin{pmatrix} y_1 & y_2 & y_3 & \cdots & y_K \\ y_2 & y_3 & y_4 & \cdots & y_{K+1} \\ \vdots & \vdots & \vdots & \ddots & \vdots \\ y_L & y_{L+1} & y_{L+2} & \cdots & y_{K+L-1} \end{pmatrix}$$

In order to obtain the principal components, we need to apply the Singular Value Decomposition (SVD) to the matrix X, which allows us to obtain the eigenvalues of the matrix XX^T, denoted by $\lambda_1, ..., \lambda_L$, and the corresponding system of orthonormal eigenvectors, $U_1, ..., U_L$, as well as the eigenvectors of $X^T X$, denoted by $V_1, ..., V_L$, which satisfy

$$V_i = X^T U_i / \sqrt{\lambda_i} \tag{1}$$

The eigenvectors can be grouped taking into account that some of them may describe a variation of the same frequency and thus they may correspond to the same principal component. In our application of the SSA technique we will find that most of the eigenvectors can be grouped in pairs to form the principal components. In order to discover the most appropiate grouping, the correlation among the contributions to the global signal by each different principal component, shown in Fig. 4, must be taken into account as explained in [9]. If two components have a very strong correlation, it means that their combination forms a principal component.

Let λ_{i_1}, U_{i_1} and λ_{i_2}, U_{i_2} be two eigenvalues and two eigenvectors that describe a variation of the same frequency and form, thus, a principal component together. Then, the contribution of this principal component to the global signal will be

$$X_{i_1,i_2} = \sqrt{\lambda_{i_1}} U_{i_1} V_{i_1}^T + \sqrt{\lambda_{i_2}} U_{i_2} V_{i_2}^T \tag{2}$$

The sum of the contributions of all the principal components will be equal to the original signal.

The normalized contribution of each principal component to the global time series of the first SR amplitude in the NS direction is shown in Fig. 5, when only one time sample is considered for each month of recordings, and in Fig. 6, when one time sample is considered for each day of recordings.

The Fast Fourier Transform of the principal components reveals the frequency content of each one of the principal components. It can be seen in Fig. 7 and in Fig. 8 when taking one sample per month and one sample per day, respectively.

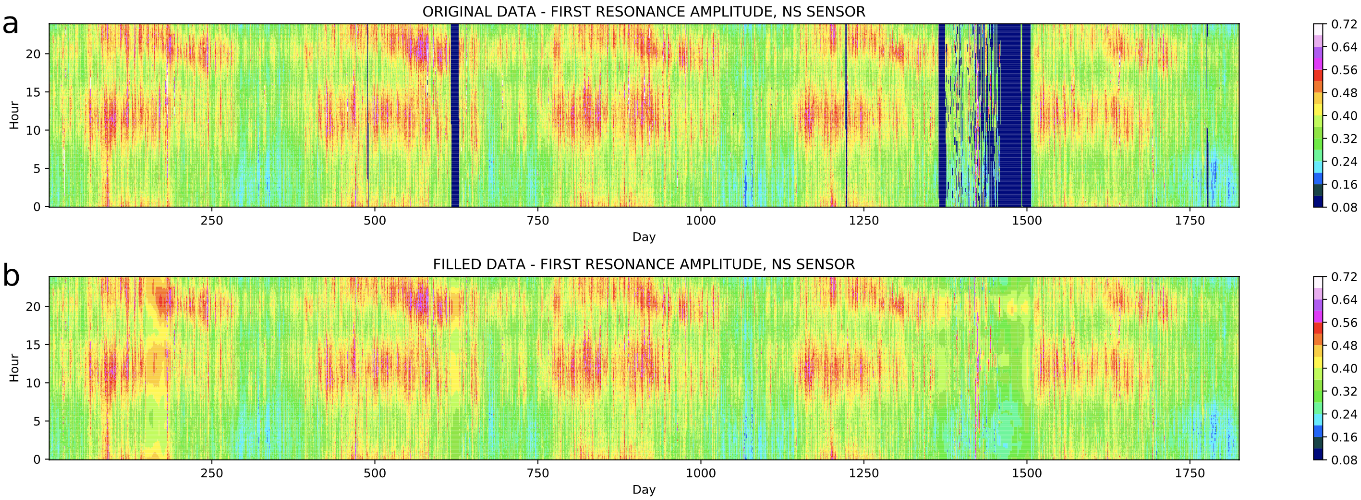

Fig. 2. (a.) Original time series of the values of the first SR amplitude for the NS sensor. The data gaps are in dark blue. Some of them last for less than one hour (we can observe them around the day 1400) and others last for approximately 40 days (between the days 1460 and 1500 approximately). (b.) Filled time series of the values of the first SR amplitude for the NS sensor. The result of the filling can be considered acceptable as the observed evolution is compatible with the evolution observed in the original data.

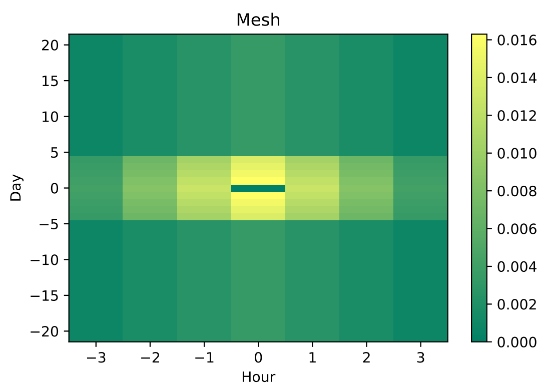

Fig. 3. Relevance given to each interval when the central value of the mesh must be filled. When a gap is short (less than 5 days) the intervals within a period of 4 days before or after the value to estimate are by far the most relevant values. For long gaps, more distant intervals have to be considered due to the lack of close intervals.

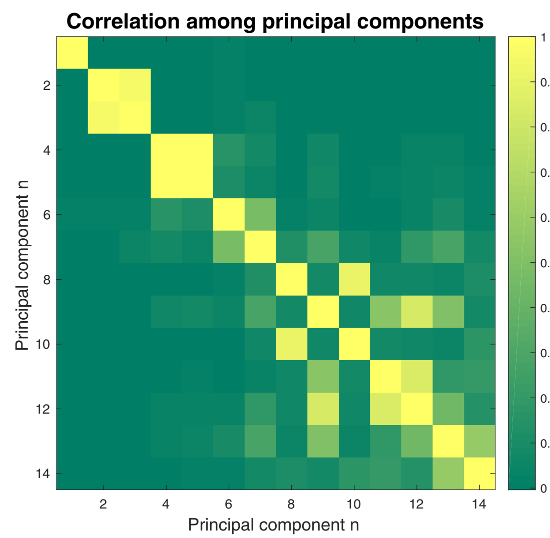

Fig. 4. Correlation among the different principal components obtained. This plot shows that the components which correspond to the a same frequency (or period) of variation are grouped in pairs (2 and 3, 4 and 5, 8 and 10, 11 and 12, 13 and 14).

IV. Results

When taking only one sample per month, as seen in Fig. 5, we can clearly observe that the components 1, 6 and 7 do not show an oscillation of the first SR amplitude, but an interannual trend. Also, the components 2 and 3, 4 and 5, 8 and 10, 11 and 12, and 13 and 14 can be grouped as they represent an oscillation of the same frequency and they show a very strong correlation. The eigenvalues for the first components can be seen in Fig. 9.

It is clear that the components 2-3 show the annual variation, and the components 4-5 show the semiannual variation of the series, as previous studies had found [1]. Their contribution to the global series is the 1%. In addition to them, the rest of the components show other scale variations. The component 9 and the components 11 and 12 show a variation with a period close to 4 months (120 days), and the components 13 and 14 show a variation with a period in the range 75-100 days, also near 8 months.

When taking one sample per day, similar results are observed, with the differences that the time resolution is higher and the grouping of the contributions of the eigenvectors is slightly different. The frequency content of the principal components is show in Fig. 7 and in Fig. 8, and it confirms these observations.

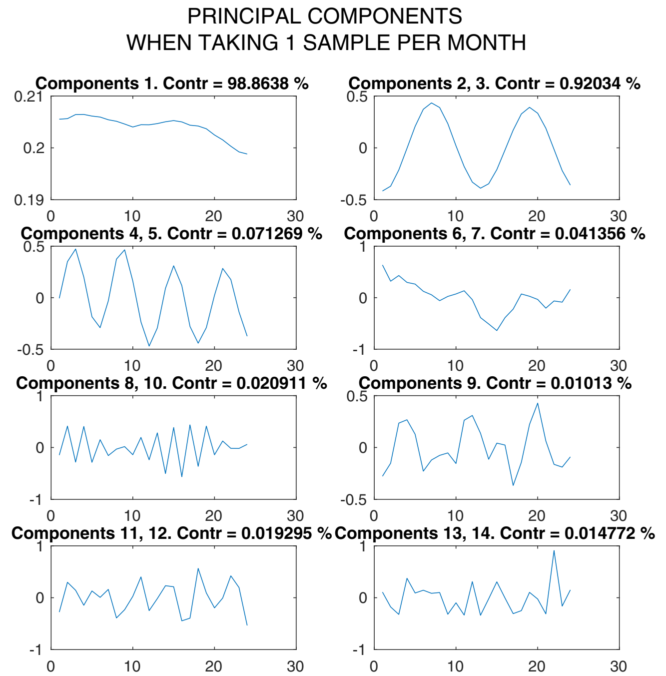

Fig. 5. Principal components obtained for the time series of the first SR amplitude in the NS direction, when only one sample per month is considered for the time series. X-axis scale is in months. Components 1 and 6-7 do not show any oscillation, but they are interannual trends. The component 2-3 show the annual component and the component 4-5 show the semiannual component. The rest of the components show minor scale variations.

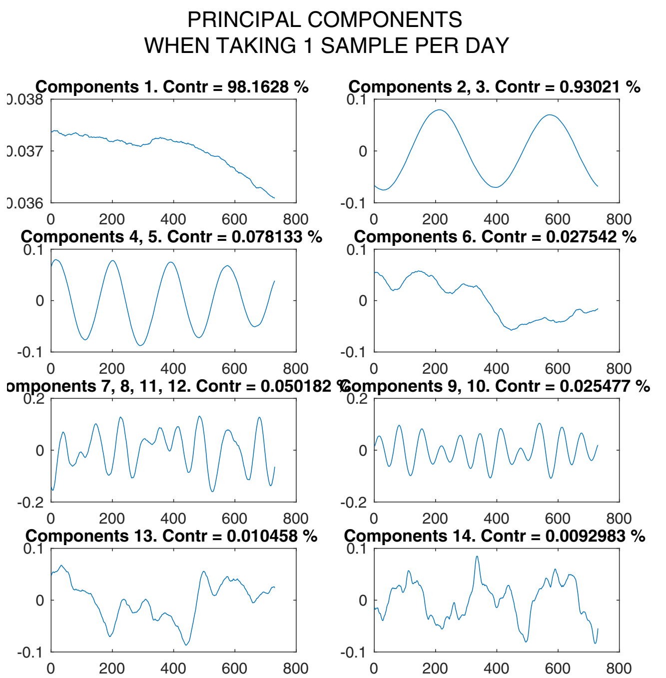

Fig. 6. Principal components obtained for the time series of the first SR amplitude in the NS direction, when one sample per day is considered for the time series. X-axis scale is in days. Components 1 and 6 do not show any oscillation. The component 2-3 show the annual component and the component 4-5 show the semiannual component. The rest of the components show minor scale variations. The result is very similar to the previous one shown in Fig. 5.

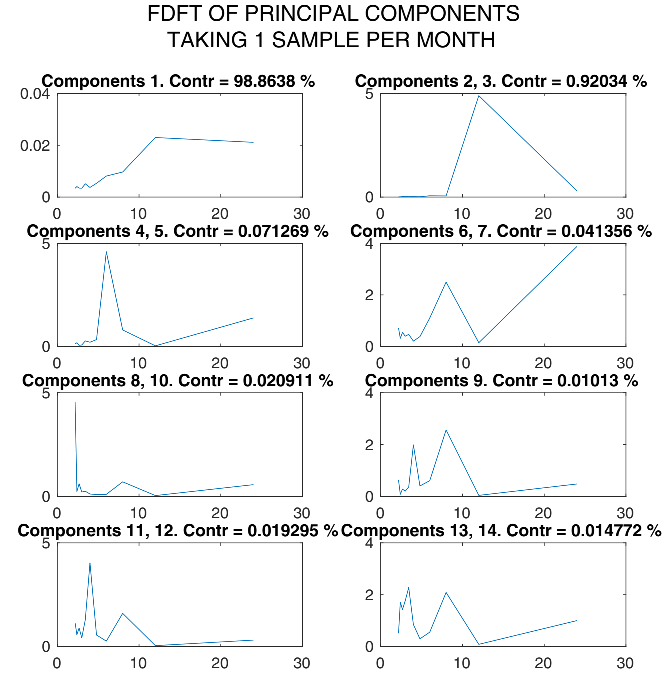

Fig. 7. Fast Fourier Transform of the principal components obtained for the time series of the first SR amplitude in the NS direction, when only one sample per month is considered for the time series. X-axis is period (the inverse of the frequency), and the unit is months. The component 2-3 has a clear content for the 12 month period, whereas the component 4-5 has a clear content for the 6 month period. The rest of the components show periods of 2-4 months, and also of 8 months.

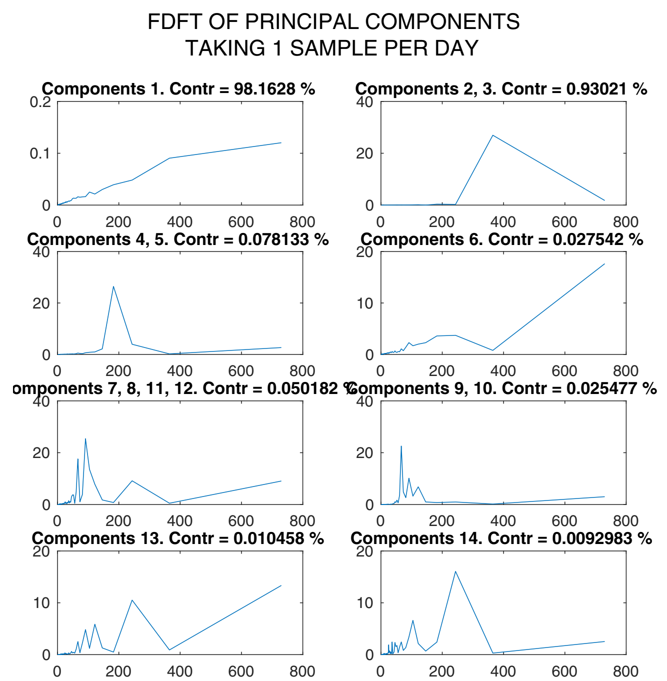

Fig. 8. Fast Fourier Transform of the principal components obtained for the time series of the first SR amplitude in the NS direction, when only one sample per day is considered for the time series. X-axis is period (the inverse of the frequency), and the unit is days. Again, the component 2-3 has a clear content for the 12 month period, whereas the component 4-5 has a clear content for the 6 month period. The components with minor contributions for periods of 2-4 appear as in the previous case shown in Fig. 7.

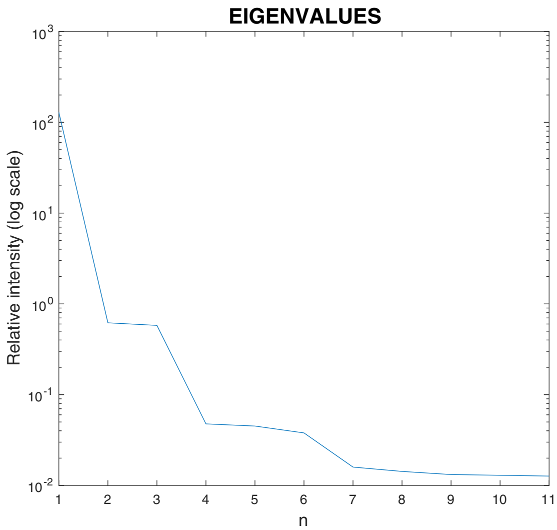

Fig. 9. Eigenvalues $\lambda_1, ..., \lambda_L$ obtained for the XX^T matrix when taking 1 sample per month for the time series. The eigenvalues show the realtive importance of the contribution of each eigenvalue U_i to the global series.

V. Conclusions

1) The SSA technique has achieved a good separation of the original first SR amplitude (NS direction) time series into smaller components that represent more interpretable variations in different time scales.
2) An annual and a semiannual component have been identified in the time series, as it had been reported in previous studies. Also, other less energetic principal components have been found with periods between 2 and 4 months, which could match the evolution of some atmospheric waves like the Madden-Julian oscillation and the Kelvin waves.
3) Similar qualitative results have been found when applying SSA to a series with 1 time sample per month, and to a series with 1 time sample per day. The time and frequency resolutions are higher when taking 1 sample per day.
4) The preprocessing of the data series, filling the gaps of data that may appear due to technical failures, is required to apply SSA. The preprocess used in this work has given an acceptable result as the evolution observed in the filled data is clearly expectable from the original data series.

References

[1] A. Nickolaenko and M. Hayakawa, *Schumann resonance for Tyros*. Springer, 2014.

[2] C. Price, E. Williams, G. Elhalel, and D. Sentman, "Natural ELF fields in the atmosphere and in living organisms," *International Journal of Biometeorology*, pp. 1–8, Feb. 2020.

[3] P. Fdez-Arroyabe, J. Fornieles-Callejón, A. Santurtún, L. Szangolies, and R.V. Donner, "Schumann resonance and cardiovascular hospital admission in the area of Granada, Spain: An event coincidence analysis approach." *Science of The Total Environment*. vol. 705, p. 135813, Feb. 2020.

[4] E.R. Williams et al., "Inversion of multi-station Schumann resonance background records for global lightning activity in absolute units," *AGU Fall Meeting Abstracts,* Dec. 2014.

[5] M. Hayakawa, A.P. Nickolaenko, M. Sekiguchi, K. Yamashita, Y. Ida, and M. Yano, "Anomalous ELF phenomena in the Schumann resonance band as observed at Moshiri (Japan) in possible association with an earthquake in Taiwan," *Natural Hazards and Earth System Sciences,* vol. 8, no. 6, Dec. 2008.

[6] J. Fornieles-Callejón, A. Salinas, S. Toledo-Redondo, J. Portí, A. Méndez, E. Navarro, and J. Ortega-Cayuela, "Extremely low frequency band station for natural electromagnetic noise measurement," *Radio Science*, vol. 50, no. 3, pp. 191–201, Mar. 2015.

[7] A. Jaramillo, A.I. Quintanar, J. Rodrguez-Camacho, M. Pazos, and C. Dominguez, "Intraseasonal Modulation of the Schumann Resonances by the MJO, CCEWs and EWs," *100th American Meteorological Society Annual Meeting, AMS,* Jan 2020.

[8] D.S. Broomhead, and G.P. King, "Extracting qualitative dynamics from experimental data." *Physica D: Nonlinear Phenomena,* 20(2-3), pp. 217–236, Jun. 1986.

[9] H. Hassani, "Singular spectrum analysis: methodology and comparison," pp. 239–257, 2007.

[10] J. Rodríguez-Camacho, J. Fornieles, M.C. Carrión, J.A. Portí, S. Toledo-Redondo and A. Salinas, "On the Need of a Unified Methodology for Processing Schumann Resonance Measurements," *Journal of Geophysical Research: Atmospheres*, vol. 123, pp. 13277–13290, Dec. 2018.

[11] J. Rodríguez-Camacho et al., "An approach for long-term study of Schumann Resonances," *In Geophysical Research Abstracts,* vol. 21, Jan. 2019.

[12] J. Rodríguez-Camacho et al., "Graphical Schemes Designed to Display and Study the Long-term Variations of Schumann Resonance," *27th European Signal Processing Conference, EUSIPCO 2019*, pp. 1–5. IEEE. Sep. 2019.